Radioactivity of Air

ENPH 453 E3 – Group 25 (Kate Szabo, Claire Floras, Julia Everitt)

April 11th, 2023

Executive Summary

The aim of this experiment was to investigate the concentrations of radioactive isotopes in the air in Stirling Hall. Radioactive radon gas tends to accumulate in poorly ventilated areas like basements, and prolonged exposure can cause potential health risks to humans [1]. A 2019 study in Kingston indicated Rn levels in residential buildings are above the threshold of safe exposure of 200 Bq/m^3, thereby motivating an investigation of the Rn concentrations in Stirling Hall [2].

The apparatus used an air sampler to collect dust particles from the air onto filter paper which was then inserted into a germanium spectrometer. The spectrometer displayed a spike in voltage when a gamma ray excited an electron inside the crystal lattice of its detector and this spike was amplified using a variable amplifier. The number of spikes with different energies were counted and displayed using a multi-channel analyzer (MCA). By measuring the gamma ray energies and decay rates of six sources with known radioactive pathways, a relationship was established between the number of counts on the MCA and the energy peaks. Using the known half-life and age of each sample, the detector efficiency as a function of gamma ray energy was determined. The volumetric flow rate of the air sampler was measured and calculated to be $(30.2 \pm 0.5) m^2/s$.

To capture radioactive particles from the air, the air sampler was placed in the basement of Stirling Hall for a 40-hour period of data collection and at the top of the stairwell for a 2-hour period. The collection times were selected based on the half-lives of decaying ^{220}Rn and ^{222}Rn. The resulting energy peaks were determined for the radioactive daughter isotope ^{214}Pb and are displayed below.

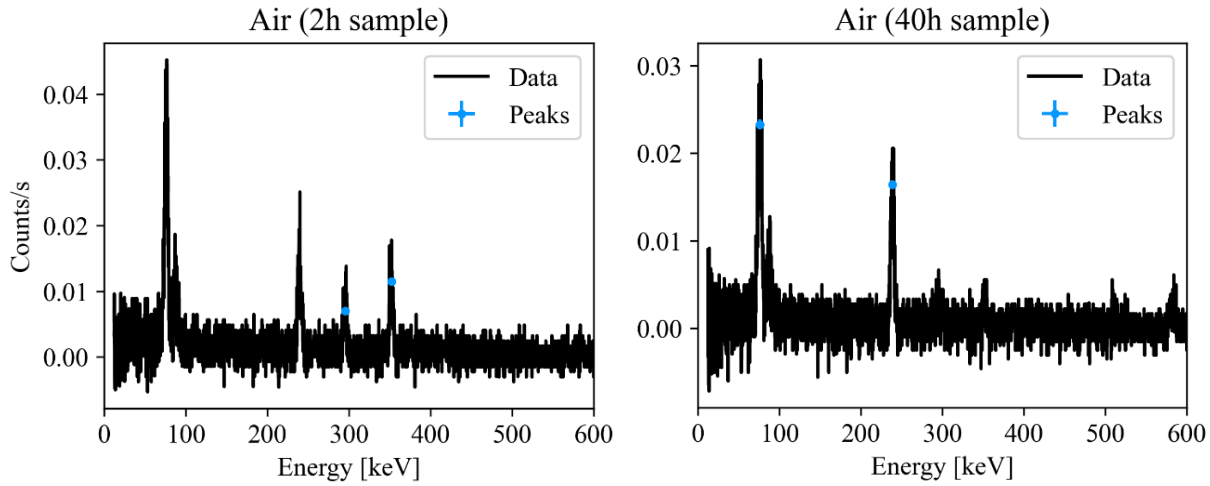

Figure: Detected gamma spectra from air samples collected over two different durations. The position and amplitude of the peaks that were analyzed are indicated in blue, where the uncertainty on the energy and rate of each emission is found based on the uncertainty of gaussian fits to each spectrum.

By using differential equations to represent radioactive growth and decay, it was possible to work backward and find the concentration of ^{220}Rn in the air in Stirling Hall to be 2 ± 2 Bq/m^3 (in the basement) and the concentration of ^{222}Rn to be 70 ± 30 Bq/m^3 (in the 6th floor stairwell). These values are on the same order of magnitude as the expected range of Rn concentrations for indoor spaces in Kingston, which is between 50 and 250 Bq/m^3, but do not match the expected result of higher radon concentrations in poorly-ventilated basement areas. The results could be improved upon by using a different method to find volumetric efficiency, improving the observation of higher energy peaks, and collecting both sets of data under the exact same conditions in Stirling Hall.

Abstract

The purpose of this experiment was to determine the concentration of radioactive isotopes in the air in Stirling Hall to investigate whether the safe exposure limit for Radon gas is exceeded. The study was motivated by a 2019 investigation which indicated that some Kingston residential buildings have radon concentrations above 200 Bq/m^3 [2]. The experiment tracked the decay of ^{220}Rn and ^{222}Rn and determined that the concentrations in the air were 2 ± 2 Bq/m^3 and 70 ± 30 Bq/m^3, respectively. While the concentration for ^{220}Rn is on the expected order of magnitude, that for ^{222}Rn is much higher than expected. Explanations for the discrepancy include that both radon measurements were conducted in different locations, inaccuracies were introduced into calculations during the measurement of the volumetric flow rate, and the measurements of higher energy peaks were inaccurate. It is recommended that the experiment be repeated under the same conditions for both measurements.

1 Introduction

Radioactivity is the spontaneous decay of unstable atomic nuclei into a more stable configuration and is a property of some naturally occurring elements and artificial isotopes [3]. During decay, electromagnetic radiation and particles can be emitted and decay into further unstable isotopes before a stable nuclide is eventually achieved. While humans are constantly exposed to low level radiation in the environment, radiation at high levels can be harmful and is a known cause of cancer [4]. Radon is a radioactive gas which often accumulates in indoor locations lacking ventilation, such as basements, mines, and water treatment plants [1]. Rn gas poses a significant health risk to humans as its concentration in the air is proportional to the likelihood of developing lung cancer over long exposure times [1]. This lab therefore aims to investigate the concentrations of Rn in the air to ensure levels are below the baseline for residential buildings of 100 Bq/m^3 established by the World Health Organization (WHO) [1]. A measurement of Rn levels is especially relevant for Kingston since a 2019 study indicates that 16% of homes in the community exceed 200 Bq/m^3 [2]. Rn itself is difficult to measure directly since it is a gas at room temperature, but its polonium and lead daughter particles can be collected as dust, analyzed, and related back to Rn concentrations to determine the radioactivity of air. Thus, by determining the amount of daughter particles in a sample after a certain time, the amount of Rn in the sampled volume of air can be determined.

2 Theory

The time taken for half a given quantity of a radioactive isotope to decay is known as the half-life and varies depending on the initial isotope. Particle emissions in radioactive decay can be classified as alpha, beta, gamma particles, or neutrons, with each type of decay occurring at a different rate and with a different branching ratio [5]. Some radioactive isotopes can decay to form daughter particles that are themselves also radioactive isotopes, thus forming a decay chain. If the radiative pathways involved in the chain are known, measurement of the concentration of daughter particles can be traced back to find the concentration of parent isotopes further up the chain [5]. Here, gamma radiation of daughter particles of ^{220}Rn and ^{222}Rn is measured, which consists of radiative emission in the form of a high-energy photon [6]. In order to relate the counts of gamma radiation to a concentration of Rn, decay rate equations are used to find the populations of parent particles based on the number of daughter particles. The population of particles in a radioactive sample, N, is described by:

$$\frac{dN}{dt} = -\lambda N \tag{1}$$

where $\lambda = 1/\tau$ is the decay rate, and τ is the mean lifetime. Solutions to Equation 1 take the form:

$$N(t) = N_0 \exp(-\lambda t) \tag{2}$$

where N_0 is the initial population at $t = 0$. In a decay chain with populations N_i, where N_{i-1} represents the parent of nuclide i, the population of particle i is affected by both growth and decay, and changes following the relationship:

$$\frac{dN_i}{dt} = \lambda_{i-1} N_{i-1} - \lambda_i N_i. \tag{3}$$

The decay rate of a particle can be calculated using its half-life using Equation 5.

$$\lambda = \frac{0.693}{t_{\frac{1}{2}}} \tag{5}$$

Where $t_{1/2}$ is the half-life of the particle.

3 Apparatus and Procedure

There were several main components of the apparatus used for all data collection as well as additional components which assisted with the calibration process. Before data could be collected, it was necessary to calibrate the apparatus to ensure the output was providing meaningful information and to calculate certain specifications detailed below.

3.1 Apparatus

The apparatus for this experiment consisted of an air sampler, gamma ray spectrometer, amplifier, multi-channel analyzer, and several supporting components, as presented in Figure 1.

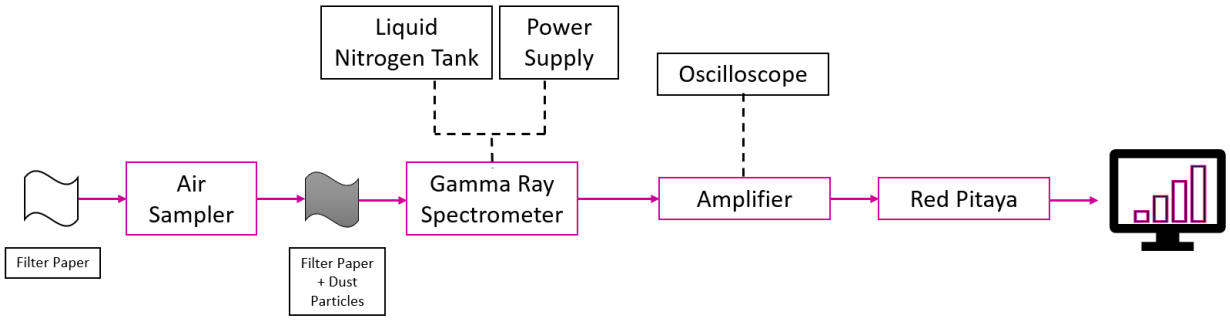

Figure 1: Schematic displaying the apparatus chronologically from left to right. Air flowed through an air sampler and small particles were collected on a filter paper, which was then placed inside the measurement apparatus. Gamma radiation was detected by a germanium spectrometer, where the resulting electrical signal was then amplified and sent to the MCA for display and further analysis.

When the air sampler was switched on, it continuously collected dust particles from the surrounding air onto a piece of filter paper for a specified length of time. The filter paper could then be removed from the sampler and inserted into a small lead-insulated cavity next to the detector of the germanium gamma ray spectrometer. Germanium spectrometers provide high resolution gamma ray detection, making them an ideal measurement device for this experiment [7]. The energy of the gamma ray is measured through photoelectric absorption in the germanium crystal, which generates a small voltage signal. The output from the spectrometer was amplified and sent to a Red Pitaya, which acted as a MCA. The MCA counted the number of voltage spikes with energies associated with a range of pre-defined bins. Thus, the

amplifier had to be carefully tuned so that the energies of interest would be in the mid-range of the MCA bins. The MCA also needed to be calibrated in order to be able to associate each bin with an actual gamma ray energy value. Table 1 contains specific information for each component of the apparatus.

Table 1: List of each component in the apparatus and corresponding descriptive information.

Component Name	**Description**
Air Sampler	General Metal Works, 120 V, 8 A, Model B/M2000H
Filter Paper	GE Healthcare Glass Microfiber Filters
Spectrometer	Gamma Ray Spectrometer run at -3.5 kV
Liquid Nitrogen Tank	EG&G Ortec Tank
Amplifier	Ortec 474 Timing Filter Amp
Power Supply	NEG HV 0-5 kV
Red Pitaya	RP-F05FF7 Local Red Pitaya
Oscilloscope	Tektronix TDS 3012B Two Channel Color Digital Phosphor Oscilloscope
Monitor	Dell Monitor

3.2 Safety Considerations

There were two major components of the lab which required special attention to safety: the spectrometer and the radioactive sources. Since the spectrometer operated at a high voltage, it was necessary to always cool the equipment with liquid nitrogen when the power supply was turned on. In all procedures for data collection and calibration outlined below, the liquid nitrogen levels in the tank were checked to be sufficient before switching on the power supply. Additionally, it was crucial that the power supply was turned off before leaving the lab.

3.3 Amplifier Calibration

To determine the correct settings at which meaningful data could be collected, it was necessary to calibrate the amplifier by following the steps below:

1. Switch on the power supply.
2. Locate and sign out a radioactive source.
3. Wearing gloves, move the outermost lead piece of the spectrometer and place the radioactive source inside.
4. Detach the connection between the amplifier and MCA, and connect the amplifier to the oscilloscope Channel 1 instead.
5. Switch on the oscilloscope and adjust the display until the signal is clearly visible.
6. Adjust the settings on the amplifier and observe the corresponding changes in the oscilloscope display. Continue to adjust the settings until the optimal signal is achieved, which appears as a sharp spike with a longer trailing end on the right.
7. Re-connect the amplifier output to the MCA, and observe the position of the gamma ray peaks in the range of the spectrum. In order to observe the desired peaks in an air sample, the MCA channels should cover at least 600 keV, but ideally show up to 1200 keV. Using the known gamma ray peak(s) as a reference, adjust the amplifier settings until the MCA bins cover the desired energy range. It may be necessary to repeat step 6 to ensure that the signal still appears in the correct shape.
8. Return the cable connections to their previous configuration and switch off the power supply.
9. Carefully remove and return the radioactive source.

This calibration process was completed once at the beginning of data collection and the optimal settings were determined to be x10 for coarse gain, x12.5 for the fine gain, 200 for integrate (nS), and 500 for diff (nS). These settings remained unchanged for the remainder of the experiment.

3.4 Red Pitaya & MCA Calibration

Calibration was required to relate the MCA channels to energy. To achieve this, six samples were chosen with known gamma peaks between 50 keV and 1300 keV. For each sample, the following steps were followed:

1. Switch on the power supply.
2. Locate and sign out the radioactive source.
3. Wearing gloves, move the outermost lead piece of the spectrometer and place the radioactive source inside.
4. Start the MCA data collection on the monitor. Allow collection to run for a minimum of five minutes to obtain a defined distribution of unitless counts.
5. Stop the MCA data collection and export the data to a CSV file.
6. Put gloves back on to remove the source from the detector.
7. Sign the source back in and repeat steps 2-6 for the next source.
8. Repeat steps 4-5 once more without a source for at least twenty minutes to obtain data on the background noise.

This data was analyzed as described in Data Analysis to determine the relationship between MCA channels and energy.

3.5 Air Sampler Calibration

It was necessary to determine the volumetric flow rate of air in the air sampler for the analysis portion of the lab, and the following procedure was used to do so:

1. Use tape to secure a 178 L garbage bag to the air sampler and record the volume of air this taped section subtracts from the total volume.
2. Cut a small hole in the garbage bag to allow air to escape and prevent the bag from popping.
3. Start a timer as the air sampler is switched on and stop the timer when the bag is completely filled with air.
4. Repeat step 3 at least 3 more times to obtain a more reliable result.
5. Use the average of all the times and the volume to calculate the volumetric flow rate.

This calculation was completed once before data collection and step 3 was repeated four times. The resulting flow rate was calculated to be 30.2 ± 0.5 m^3/s with the error estimated based on inaccuracies in timing and in the measurement of how much the taped section of the bag detracted from the total volume.

3.6 Data Collection Procedure

Once the MCA was calibrated, data collection could begin.

1. Unscrew the backing on the air sampler and place one piece of filter paper on top of the mesh before screwing it back on.
2. Bring the air sampler to the chosen location – for a short data collection the top of the stairwell in Stirling Hall is a suitable location, and for a long data collection the basement is suitable. Place the sampler on its side with the filter paper sitting vertically, in order to ensure that the air sampler opening is not blocked. Plug in the air sampler and make a note of the time.

3. Allow the sampler to run for the chosen amount of time, approximately 2 hours for detection of ^{222}Rn and 40 hours for ^{220}Rn. These times were determined based on the half lives of the daughter particles of interest. ^{220}Rn has a daughter particle with a half life of 10.64 hours, while the daughter particles of interest for ^{222}Rn have half lives less than 30 minutes.
4. Turn the air sampler off and record the time. Walk with the air sampler back to the lab setup.
5. Crumple up the filter paper with dust particles collected and insert it into the spectrometer using gloves.
6. Turn on the detector, record the time, and begin collecting data on the MCA.
7. Collect data for 30 minutes and export the data files. A collection time that is significantly shorter will not allow for observation of the gamma peaks for daughter particles, and a collection time that is significantly longer will result in less clear peaks as the strength of the source and therefore relative signal decrease.
8. Wearing gloves, remove the filter paper from the spectrometer.
9. Turn the MCA back on for at least ten minutes to record the background data.
10. Export the data and turn off the apparatus.

This procedure was followed for both the short collection and long collection durations.

4 Data Analysis

4.1 Measurement Calibration

In order to determine the correlation between the MCA bins and the detected energy, gamma spectra from six different radioactive samples were measured, and the positions of the known peaks were recorded. Equation 2 was used to determine the current strength of each source based on the original value on the datasheet. The spectra and peaks of the six samples that were used for calibration are shown in Figure 2.

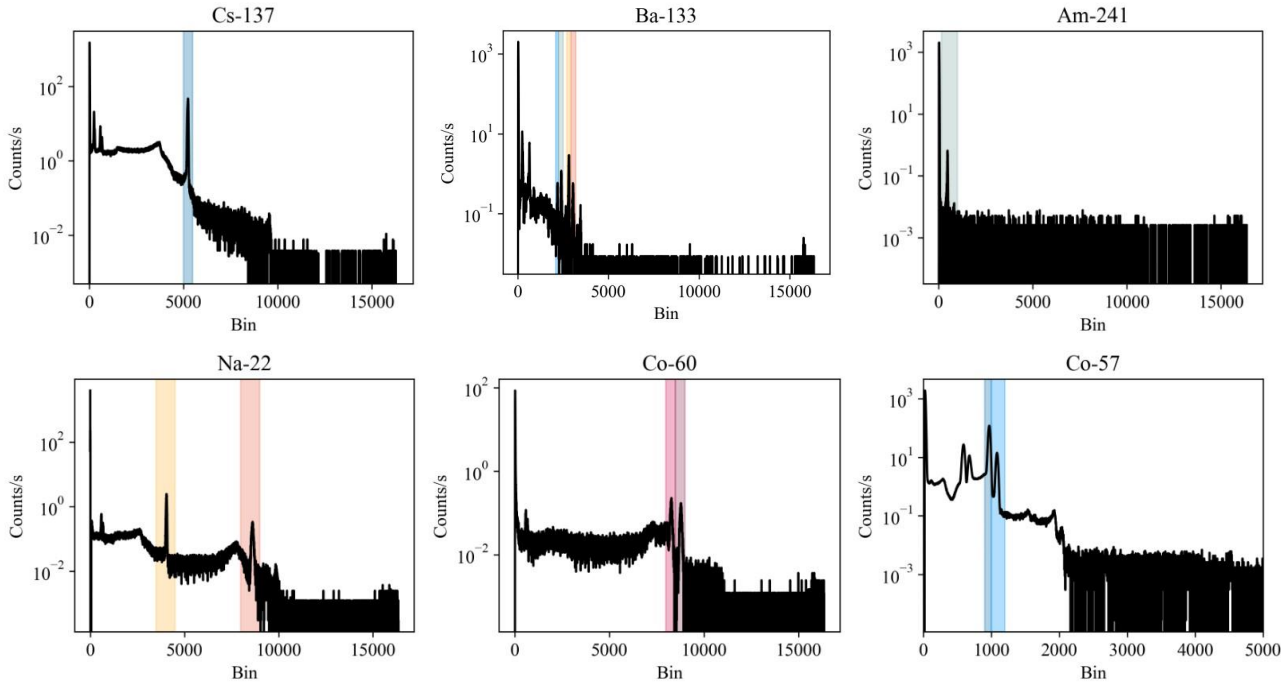

Figure 2: Gamma spectra of samples with known radiative pathways. Peaks (highlighted in colour) were identified visually, and the position and amplitude of each peak was found by searching for the maximum emission rate in each highlighted range. The uncertainty on the detected counts was taken as a poisson uncertainty of $\sqrt{N}$, where N is the number of counts in each channel.

Note the presence of two low-energy peaks in each spectrum below bin 1000. Due to possible interference with these erroneous peaks, the single detected low-energy peak of the Am-241 sample was deemed highly uncertain, and was not included in further analysis.

Due to the limited availability of high-energy sources, a pulser was also used to understand the relationship between detected energy and MCA bin above bin 10000. With the pulser at the lowest energy settings, the amplitude of a pulse was measured with the oscilloscope to be (500 ± 30) mV. This base energy could then be amplified to create pulses with higher energies.

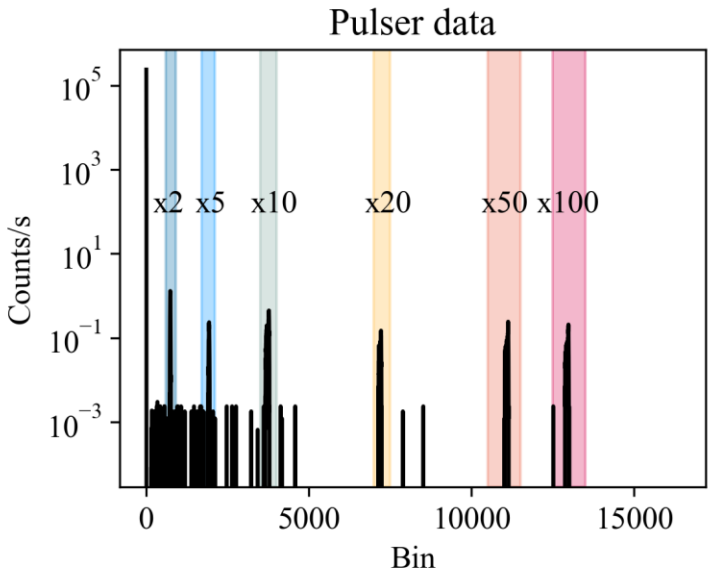

Figure 3: Peak detection for data acquired from electronic pulser. A reference pulse of 500 mV was amplified as indicated in the plot annotations. The absolute energy associated with each pulse is unknown, as each pulse contains an unknown number of electrons.

Plots of the peak positions and their known energies for the various radioactive samples and the pulser are shown in Figure 4. It should be noted that the pulses detected from the pulser contain an unknown number of electrons, so the absolute value of the pulse energy (converting V to keV) is not comparable to the gamma spectrum peak energies that are seen from the samples. These energies can only be used to observe the nature of the relationship between MCA channel and energy.

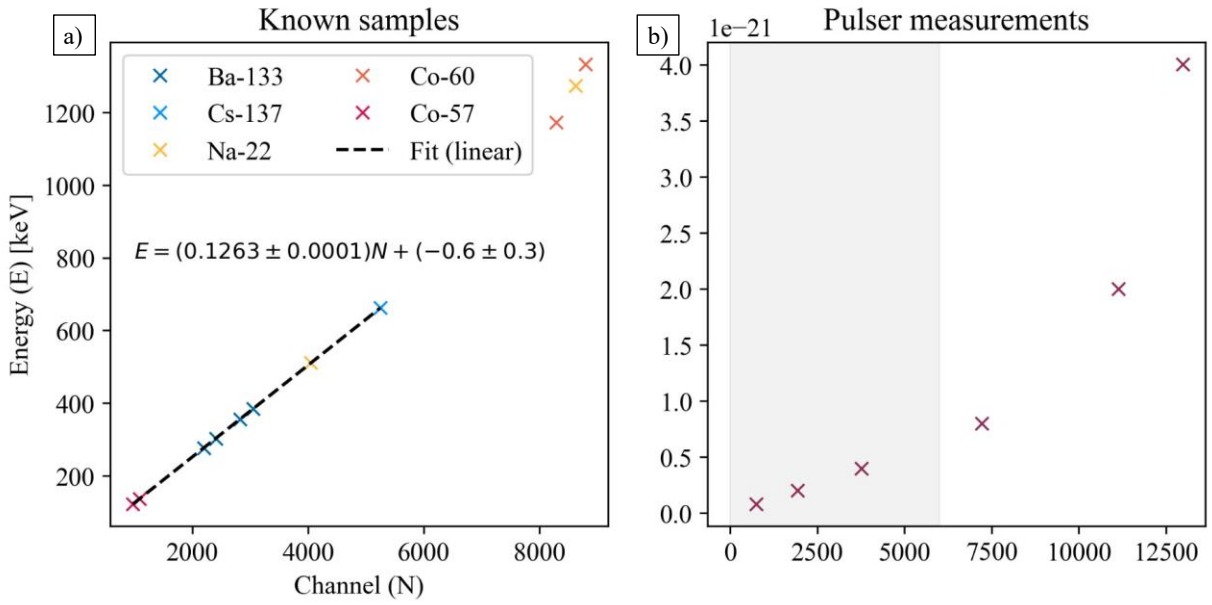

Figure 4: a) Plot showing correlation of MCA channel number with energy for a variety of samples with known gamma spectra. A linear regression was performed for peaks smaller than 800 keV, yielding a slope of $m = 0.1263 \pm 0.0001$ keV/bin with an R^2 value of 0.999997, indicating a very strong linear correlation. b) Pulser energy measurements over a much wider range of MCA channels, confirming the non-linear nature of the bin-energy correlation for higher energies. The grey region indicates the range in which the relationship is assumed to be linear.

The germanium spectrometer that was used to detect the gamma rays is known to have a non-linear efficiency in terms of the energy of the incident radiation [8]. In order to determine the efficiency of the detector, the expected decay rate for each peak of each calibration sample was identified in terms of the pathway's branching ratio and the known age and half-life of each sample. These were compared to the detected decay rate to identify the efficiency of the detector for each peak energy, shown in Figure 5.

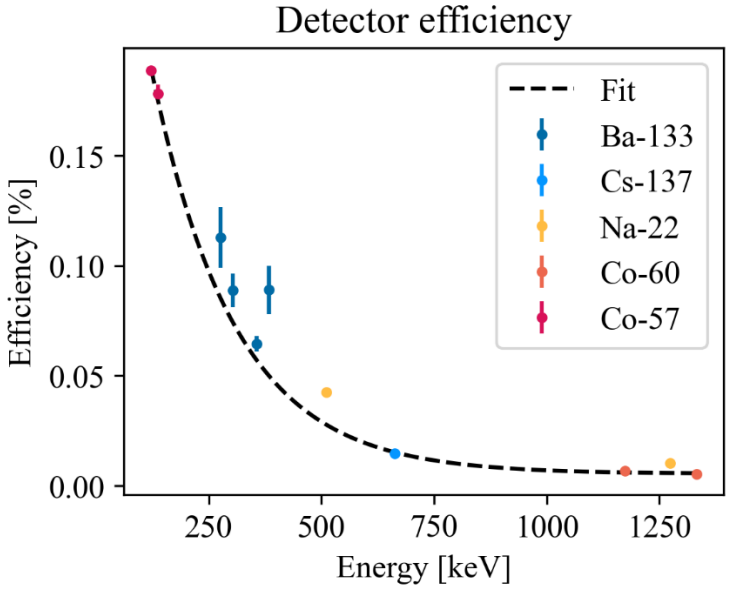

Figure 5: Efficiency of the germanium detector in terms of the energy of the incident radiation, fit with curve $\eta = a\,exp(-bE) + c$ with an R^2 of 0.93, indicating a relatively strong exponential correlation.

The efficiency of the detector was identified through curve fitting to be $(0.35 \pm 0.2)\exp(-(0.0054 \pm 0.0002)E) + (0.0055 \pm 0.0007)$. This relationship was used to determine the true number of decays associated with each gamma peak in the spectra detected from the air samples.

4.2 Air Gamma Spectrum Analysis

Gamma spectra from the air sample for two different sample times were measured, with each sample being placed inside the detector for a total of 30 minutes. The two different detected spectra are shown in Figure 6, where the four ^{214}Pb gamma ray peaks that were used moving forward are indicated in blue. The position and amplitude of each peak was found by fitting a gaussian to a segment of the spectrum near the position of the expected peak.

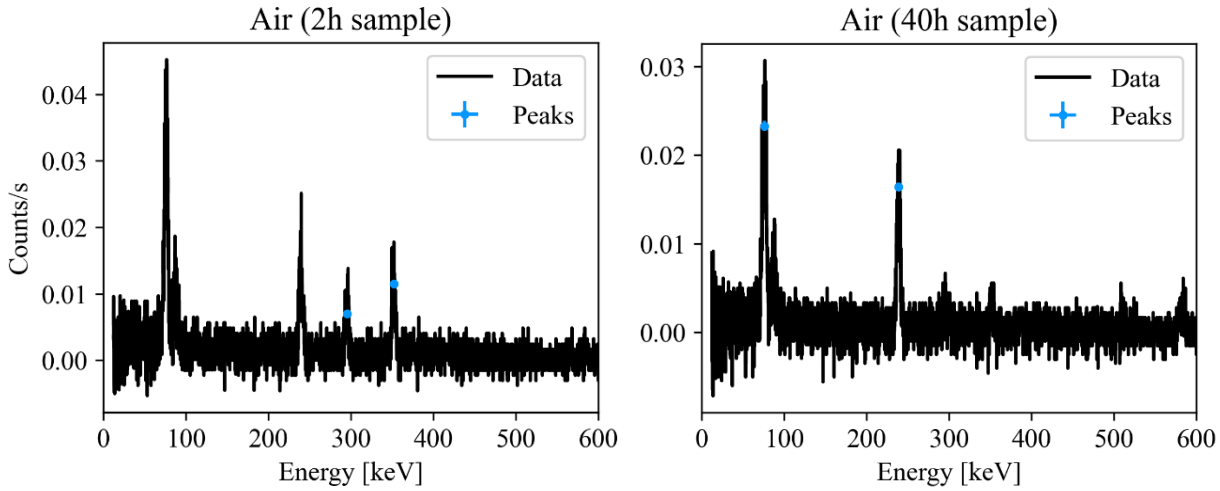

Figure 6: Detected gamma spectra from air samples collected over two different durations. The position and amplitude of the peaks that were used for further analysis are indicated in blue, where the uncertainty on the energy and rate of each emission is found based on the uncertainty of gaussian fits to each spectrum. Each peak is associated with a different decay gamma ray from ^{214}Pb with different branching ratios and half-lives.

Detailed plots and information relating to the gaussian fits is included in Appendix A. The resulting detected peaks are summarized in Table 2.

Table 2: Detected position and amplitude of gamma ray peaks from decay of 214Pb in two different air samples.

Sample	Peak energy [keV]	Decay rate [counts/s]
2h	295.39 ± 0.15	0.0072 ± 0.0004
2h	351.9 ± 0.1	0.0115 ± 0.0004
40h	76.17 ± 0.07	0.032 ± 0.001
40h	239.31 ± 0.09	0.0136 ± 0.0005

The decay rate values could then be used in combination with the detector efficiency, sampling time, and measurement time to work backward to find the concentration of each radon isotope in the air.

4.3 Radon Concentration Calculations

Equations 1 and 3 were applied to determine the amount of a given daughter particle present on the filter paper at the time the air sampler was turned off, the concentration of this particle in air, and finally related to the concentration of Rn in air using branching ratios. This was repeated for several daughter particles to provide an estimate of accuracy. A sample of this procedure for the 77 keV peak of the ^{212}Pb daughter particle in the ^{220}Rn collection is seen below.

First, Equation 1 was used to determine the amount of ^{212}Pb on the filter paper at the time the air sampler was turned off. The amount at the time of measurement with the spectrometer was determined to be 0.03 ± 0.2 decays/s, correctly expressed as 0.0 ± 0.2 decays/s, from observed gamma spectra. Using this quantity, a detector efficiency of 0.17% at 77 keV, a time of 3.3 minutes to bring the air sampler from the collection location to the lab, and decay constant of 0.0011 minutes^{-1} gives a ^{212}Pb quantity of 17.53 decays/s at the time the sampler was stopped.

$$\begin{aligned} B\left(t_{samplerStopped}\right) &= B\left(t_{spectrometer}\right)(1 + \lambda_b * t_{transport}) \\ &= \left(0.03\frac{decays}{s}\right)/0.17\%(1 + 0.0011\ min^{-1} * 3.3\ min) \\ &= 17.53\frac{decays}{s} \end{aligned}$$

Here, B is the amount of the ^{212}Pb on the filter paper, $t_{samplerStopped}$ represents the time the air sampler was stopped, $t_{transport}$ represents the time taken to bring the stopped sampler to the lab, and $t_{spectrometer}$ represents the time at which the sample was measured in the spectrometer.

Equation 3 can be written in terms of the volumetric flow rate and concentration as follows:

$$\frac{dB}{dt} = \epsilon_f \rho_b V - \lambda_b B \tag{5}$$

Where ϵ_f is the retention efficiency of the filter provided by the product specifications, V is the volumetric flow rate, and λ_b is the decay constant for the particle. Solving this differential equation gives Equation 6.

$$B(t) = \frac{V\epsilon_f \rho_b}{\lambda_b}\left(1 - e^{-\lambda_b t}\right) + ce^{-\lambda_b t} \tag{6}$$

Here, c is a constant of integration. Applying the conditions $B(0) = 0$ and $B(2770\ mins) = 17.53\frac{decays}{s}$ as determined in the previous step and isolating for ρ_b gives a ^{212}Pb concentration in the air of 0.0007 $\frac{Bq}{m^3}$. Finally, this result was divided by the branching ratios of 17.5% and 0.0018% for Po to Pb and Rn to Po, respectively, to give a ^{220}Rn concentration of 210 $\frac{Bq}{m^3}$.

The calculated values for ^{222}Rn and ^{220}Rn using this method are summarized in Table 3 below.

Table 3: Summary of the calculated Radon concentrations using various daughter particles.

Daughter Particle	Gamma Peak [keV]	Calculated Radon Concentration $[Bq/m^3]$	Sample Time	Isotope
^{214}Pb	295.2	99.34	2 hour	^{222}Rn
^{214}Pb	351.9	46.74	2 hour	^{222}Rn
^{212}Pb	77.1	3.53	40 hour	^{220}Rn
^{212}Pb	238.6	0.30	40 hour	^{220}Rn

The true concentration of Rn for each sample was taken to be the average of the values obtained using the different daughter particles. This method yielded large uncertainties due to the difference in calculated values.

5 Results and Discussion

After performing the above procedures and analysis, the concentration of ^{220}Rn was determined to be 2 ± 2 Bq/m^3 and the concentration of ^{222}Rn was determined to be 70 ± 30 Bq/m^3 in the air in Stirling Hall. The expected range of radon concentrations for indoor spaces in Kingston was between 50 and 250 Bq/m^3, with higher values expected in poorly ventilated areas based on the results of a 2019 study in the region. The measurement for ^{222}Rn therefore makes sense with this expected range; however, the calculated value for ^{220}Rn is significantly lower than the expectation with a large error. It should also be noted that the ^{220}Rn measurement was conducted in the basement, where poor ventilation often causes higher radon concentrations, but this trend was not observed in these measurements. Instead, the measured ^{222}Rn concentration on the 6th floor of Stirling Hall was found to be higher than that of the basement. These measurements suggest that the risk of Rn exposure in Stirling Hall is acceptable within guidelines. However, given the large uncertainty and deviation from expected trends, it is recommended that the measurements are repeated before health recommendations are provided.

The accuracy of the Rn concentration calculation could be improved by applying more complex differential equations to relate the concentration of Pb to Rn rather than by using branching ratios alone. Another method, such as obtaining a value directly from the manufacturer, could also be used to re-calculate the volumetric flow rate of the air sampler. Uncertainty in the volumetric flow rate impacts calculations differently depending on the length of collection time, and thereby has the potential to skew results taken over longer durations. By determining a more accurate flow rate and comparing results with the chosen method in this experiment, an overall result with improved accuracy could be obtained. In addition, observation of gamma spectra was limited at higher energies, as evidenced by the non-linearity in the plot showing the correlation between MCA channel number and energy. This potential discrepancy in the results due to detector efficiency could be improved upon by tuning the amplifier settings to obtain clearer results at higher energies. This improvement would allow the expected Po peak around 800 keV to contribute to results.

6 Conclusion

Elevated concentrations of radioactive substances such as radon in the air are concerning to human health, and thus measurement of the radioactivity of air is key to determining the safety of a workplace such as Stirling Hall. Here, concentrations of ^{220}Rn and ^{222}Rn in the air in the basement and 6th floor stairwell of Stirling Hall were determined through detection of daughter particles in collected dust samples at each location. Dust particles were collected on sheets of filter paper placed on the opening of an air pump with a measured volumetric flow rate of $(30.2 \pm 0.5) m^2/s$. Daughter isotopes of ^{222}Rn ($t_{1/2} = 30\ mins$) were measured after a sampling period of 2 hours, and daughter isotopes of ^{220}Rn ($t_{1/2} = 10.64\ hrs$) were measured after sampling the air for 40 hours. Gamma radiation from each filter paper was detected using a germanium spectrometer that generated a spike in voltage when a gamma ray excited an electron inside the crystal lattice of the detector. This spike was amplified by a variable amplifier, and the number of spikes with different energies were counted and displayed by a multi-channel analyzer. The energy range and efficiency of this measurement system was calibrated through measurement of the gamma ray energies and decay rates from six different radioactive samples with known radiative pathways.

Gamma ray peaks associated with various gamma decays from daughter isotope ^{214}Pb were identified at their expected energies from each of the two different air samples. The decay rates for each of these peaks were found by fitting a gaussian to each peak. These decay rates, along with the determined detector efficiency, volumetric flow rate, duration of sampling and measurement, and known branching ratios for the radiative pathways from ^{220}Rn and ^{222}Rn were then used to work backward to find the initial

concentrations of each Rn isotope in the air. The concentration of ^{220}Rn in the 6th floor stairwell of Stirling Hall was determined to be 2 ± 2 Bq/m^3, and the concentration of ^{222}Rn in the basement of Stirling Hall was determined to be 70 ± 30 Bq/m^3. The concentration of ^{222}Rn falls within the expected range of 50-250 Bq/m^3, but the final determined concentration of ^{220}Rn does not fall within the expected value, and has an extremely high relative uncertainty. Possible reasons for this discrepancy include error in the volumetric flow rate calculation, limitations in detector efficiency at higher energies, and the varied locations of measurement. Although the Rn concentrations calculated in Stirling Hall are below the safe exposure threshold for indoor Rn concentrations, it is recommended in future that each of the potential problems identified be addressed and data collection be repeated to obtain a more reliable result that can better inform the level of health risk Rn poses.

References

[1] World Health Organization, "Radon," 25 01 2023. [Online]. Available: https://www.who.int/news-room/fact-sheets/detail/radon-and-health. [Accessed 14 03 2023].

[2] City of Kingston, "Radon Gas Mitigation," [Online]. Available: https://www.cityofkingston.ca/resident/building-renovating/radon-gas-mitigation#:~:text=Radon%20gas%20in%20Kingston,gas%20of%20200%20Bq%2Fm3. [Accessed 14 03 2023].

[3] J. O. Rasmussen, E. P. Steinberg and Editors of Encyclopaedia Britannica, "radioactivity," 24 03 2023. [Online]. Available: https://www.britannica.com/science/radioactivity. [Accessed 28 03 2023].

[4] A. Z. a. C. Hardiman, "Electromagnetic Radiation and Human Health: A Review of Sources and Effects," *High Frequency Electronics,* vol. 4, no. 3, pp. 16-26, 2005.

[5] Centers for Disease Control and Prevention, "What is Radiation? Properties of Radioactive Isotopes," Centers for Disease Control and Prevention, 20 August 2015. [Online]. Available: https://www.cdc.gov/nceh/radiation/isotopes.html#:~:text=Radioactive%20decay%20is%20the%20process,the%20radiation%20it%20gives%20off.. [Accessed 11 April 2023].

[6] J. Donev, "Energy Education," University of Calgary, [Online]. Available: https://energyeducation.ca/encyclopedia/Gamma_decay#:~:text=Gamma%20decay%20is%20one%20type,gamma%20ray%20photon%20%2D%20is%20released.. [Accessed 11 April 2023].

[7] K. Buchtela, "Gamma Ray Spectrometry," ScienceDirect, 2005. [Online]. Available: https://www.sciencedirect.com/topics/earth-and-planetary-sciences/gamma-ray-spectrometry. [Accessed 10 April 2023].

[8] F. Gao, L. W. Campbell, R. Devanathan, Y. L. Xie, Y. Zhang, A. J. Peurrung and W. Weber, "Gamma-ray interaction in Ge: A Monte Carlo simulation," *Nuclear Instruments and Methods in Physics Research B,* vol. 255, pp. 286-290, 2007.

Appendix A: Gaussian peak detection

Gaussian fits for each of the peaks of interest in both the 2h and 40h air sample measurements are included in Figure A1. Uncertainties in the position (energy) and amplitude (counts/s) of each gaussian was taken from the covariance matrix of the final fit. Fit range was adjusted until the maximum R^2 value was obtained for the given fit.

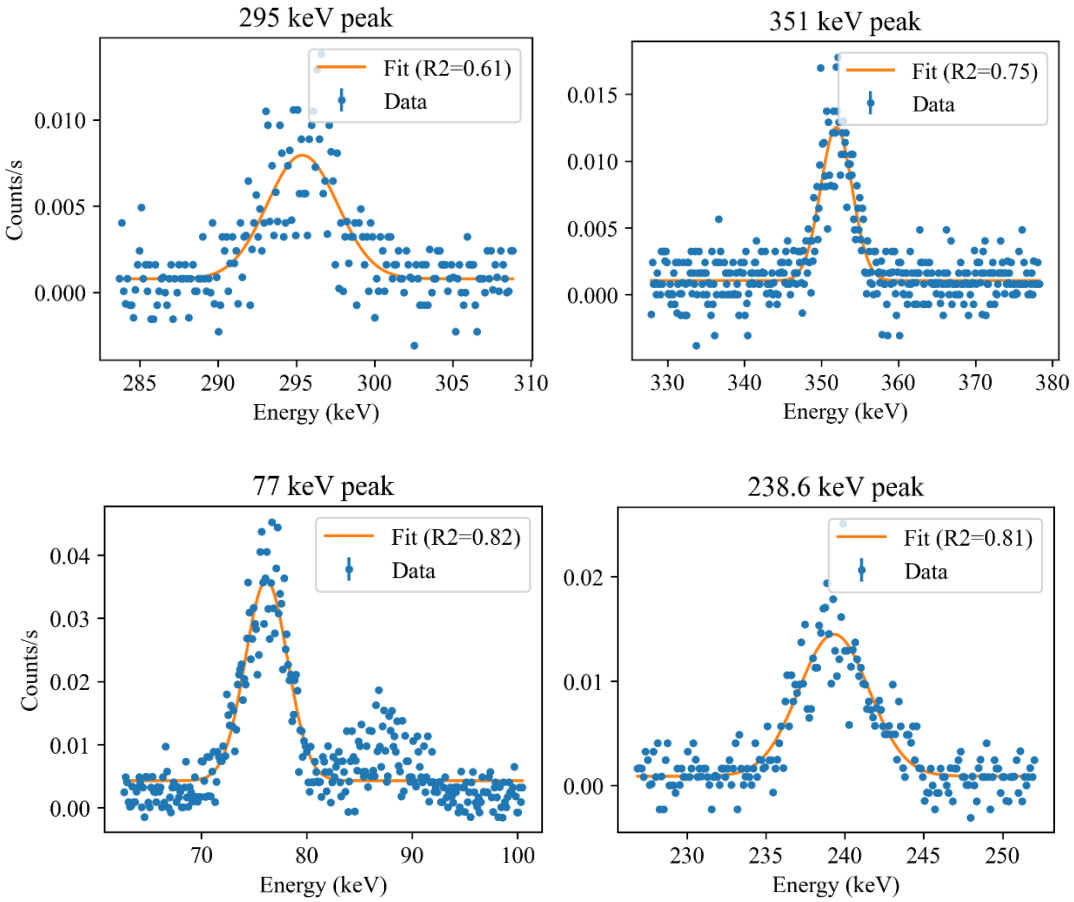

Figure A1: Gaussian fits for each of the ^{214}Pb peaks of interest in the captured air samples.